Fuel 359 (2024) 130499

Contents lists available at ScienceDirect

Fuel

journal homepage: www.elsevier.com/locate/fuel

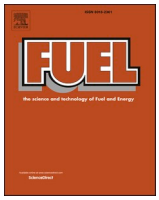

Full Length Article

A new ternary diagram to decipher the evolution of maturity and biodegradation of crude oil using ESI FT-ICR MS

Dongyong Wang [a,b], Meijun Li [a,b,c,*], Jianfa Chen [a,b], Haochen Chen [a,b], Quan Shi [d]

[a] National Key Laboratory of Petroleum Resources and Engineering, China University of Petroleum (Beijing), Beijing 102249, China
[b] College of Geosciences, China University of Petroleum (Beijing), Beijing 102249, China
[c] Faculty of petroleum, China University of Petroleum-Beijing at Karamay, Xinjiang 834000, China
[d] State Key Laboratory of Heavy Oil Processing, College of Chemical Engineering and Environment, China University of Petroleum (Beijing), Beijing 102249, China

ARTICLE INFO

Keywords:
Maturity assessment
Biodegradation degree definition
FT-ICR MS
NSO compounds
Ternary diagram

ABSTRACT

The nitrogen-, sulfur- and oxygen-containing (NSO) compounds widely occurred in crude oil and source rock extract, which could provide useful information for maturity and the degree of biodegradation. In this paper, NSO heteroatom compounds of crude oils with a series of different levels of maturations and biodegradation were analyzed by the ESI FT-ICR MS under a negative mode, and the variations of the relative abundance of those compounds were investigated. The changes of relative content nitrogen- and oxygen-containing compounds in oils with the increasing of maturity and biodegradation degree in the ternary diagrams of DBE = 9, 12 and 15 of N_1 species, DBE = 12, 15 and 18 of N_1 species and DBE = 4, 5 and 6 of O_1 species show similar tendency, which is restricted to solely characterizing the evolution of either maturity or biodegradation degree of crude oil. A new ternary diagram composed of N_1, O_1, $O_2 + O_3 + O_4$ species was presented to simultaneously distinguish the evolution of maturity and biodegradation of crude oil. Data points with high maturity oil tend to shift to N_1 species end-member, showing that the relative content of N_1 species increases and that of O_2 species decreases with increasing maturity as a consequence of decarboxylation and dehydration. Oils with high degrees of biodegradation shift to $O_2 + O_3 + O_4$ species end-member, indicating that the relative content of N_1 species decreases and that of $O_2 + O_3 + O_4$ species increases with increasing biodegradation level which may be due to the formation of organic acids in degraded oil. Therefore, the ternary diagram with three end-numbers of N_1, O_1, $O_2 + O_3 + O_4$ species is a useful tool to delineate the evolution of maturity as well as to estimate biodegradation degree.

1. Introduction

The thermal maturity of source rock refers to the degree of the chemical reactions transforming sedimentary organic matter (i.e. kerogen) to oil and gas [1–3]. The maturity is crucial for petroleum generation and accumulation, which influence the quality and quantity of hydrocarbons [4,5]. With increasing maturity, the petroleum compositions bring about marked changes, and the oil compound species, in turn, they could also be used to define the thermal maturity of petroleum [6,7]. Among those compounds, saturated hydrocarbons are essential components and have been widely applied for maturity assessment. The related saturated hydrocarbons parameters e.g. C_{31}-hopane 21S/(S + R), C_{29}-sterane ααα/(ααα + αββ) and C_{29}-sterane S/(S + R), are available when the source rock and oil are at low-medium mature stages and will reach equilibrium points to remain unchanged for samples beyond peak oil generation [8,9]. Many aromatic hydrocarbon indicators for maturity assessment, e.g. methylphenanthrene index and 4-/1-methyldibenzothiophene, have been reported, which are useful for condensate and light oil with a high maturity [4,5,10]. The saturated and aromatic hydrocarbons cannot indicate the maturity differences due to the influence of depositional environment, organic matter source, thermal maturation as well as secondary alteration [11–13]. While, the relative content of non-hydrocarbons in crude oil increases with increasing biodegradation level [14]. Metallic porphyrins, a series of trace compounds with high boiling point, mainly occur in the heavy oil and have been used to define maturity [15,16]. Even so, the porphyrins in sediments and oils are not understood due to very limited distribution and low content [17]. The NSO compounds are characterized by strong

* Corresponding author.
E-mail address: meijunli@cup.edu.cn (M. Li).

https://doi.org/10.1016/j.fuel.2023.130499
Received 1 July 2023; Received in revised form 25 November 2023; Accepted 25 November 2023

polarity and high molecular weight resulting in the difficult separation of those compounds by routine analytical tools, e.g. gas chromatography–mass spectrometry (GC–MS) and gas chromatography–mass spectrometry/mass spectrometry[6,7,18], which has severely limited the advances on NSO compounds for maturity assessment [19].

In recent years, the high-resolution mass spectrometry technology, for example, the widely used electrospray ionization (ESI) Fourier transform ion cyclotron resonance mass spectrometry (FT-ICR MS), provides an effective tool to detect non-hydrocarbon components [20–24]. In general, the FT-ICR MS offers the highest available broadband mass resolution, mass resolving power, and mass accuracy, which allows the assignment of a unique elemental composition to each peak in the mass spectrum. Thousands of compounds can be observed in the mass spectrum from FT-ICR MS. The mass ranges can be up to ~ 1500 Da for "heavy ends" in crude oil especially some heavy oils characterized by FT-ICR MS, which is far beyond what traditional mass spectrometry tools can define. More than 17,000 different elemental compositions for organic bases and acid in crude oil can be resolved and identified using high-resolution ESI FT-ICR MS of petroleum [25]. Determining a unique elemental composition for any molecule is available due to a different mass defect for every isotope of every element, which requests a sufficiently accurate mass measurement [26]. Indeed, the FT-ICR MS can measure a molecule with ~ 0.0003 Da for molecules up to ~ 1,000 Da in mass, which can be applied to uniquely determine its elemental composition from its mass alone [27]. However, the GC–MS tool can only define a molecule, which is accrate to one decimal places in mass (~0.1 Da). For example, one of the most important close doublets is molecules whose elemental compositions differ by $^{12}C_3$ vs. $^{32}SH_4$ (mass differences 3.4 mDa) [27], which requests a resolution over 150,000 if identifying those two compositions in the 500 Da mass scale [28]. Therefore, FT-ICR MS is characterized by sufficiently high mass resolving power ($m/\Delta m_{50\%}$ ~400,000, where m is molecular mass and $\Delta m_{50\%}$ is the mass spectral peak width at half-maximum peak height) [27], which can provide more elemental compositions information in a limited mass scale compared with GC–MS. This technique is useful but it has its limitations. One of the challenging problems for the present high-resolution mass spectrometry analysis is limited to compositional possibilities due to the occurrence of a large number of isomers corresponding to a given elemental compositions [29]. On the other hand, the information about the structure of NSO compounds provided by the FT-ICR MS analysis may be limited because numerous compounds may have the same molecular formula. Besides, quantitation remains still the most difficult task for mass-based petroleomics as no single ionization method produces ions from different analyte neutrals with equal efficiency [30]. Therefore, in this study, only the structures of some simple and accepted compounds were presented, such as the N_1 species with DBE = 9, 12 and 15 likely referring to carbazole analogues. The ionization efficiency is considered to be approximately equal for each sample due to the stable instrument condition. The relative abundance of major NSO-containing compounds rather than absolute content was observed and analyzed. In addition, the results presented in this work solely was based on the polar and acid compounds. For example, the basic nitrogen-containing compounds only can be ionized in a positive model and were not included due to a low content relative to neutral nitrogen.

Compared to metallic porphyrins and the biomarkers of saturated and aromatic hydrocarbons, the NSO compounds, widely occurred in various sediment and oil samples (e.g. normal oil, heavy oil, light oil as well as condensate), can applied for maturity assessment from immature to late mature stage and are barely affected by source and sedimentary environment [31]. Therefore, numerous authors provided many maturity indicators based on the compositions of acid and polar NSO compounds characterized by ESI FT ICR MS [32–39]. For example, Poetz *et al.* (2014) found that the mean DBE (Double Bond Equivalents) values of N_1 species increase with increased maturation and then proposed that the ternary diagrams of *ortho*-fused (DBE = 12, 15 and 18) and *ortho*- and *peri*-fused (DBE = 17, 20 and 23) carbazoles were promising tools for maturation assessment [34]. The unresolved complex mixture observed in the gas chromatography initially were used to determine that the oil sample have been biodegraded [40]. Five biodegradation degrees, i.e. very slight, slight, moderate, heavy and severe biodegradation, were defined based on the sequence of the removal of biomarkers [41]. Then, on a basis of the same principle, Peters and Moldowan (2005) reported a biodegradation index (PM idex), which ranks the biodegradation on a scale of 1–10 [7]. However, the above indicators merely qualitatively describe the biodegradation degrees based on biomarker from saturated and aromatic hydrocarbons. The contents of metallic elements such as nickel and vanadium increase with the increasing of biodegradation levels [42]. Up to now, the significant biodegradation of porphyrins is not confirmedly reported [7]. Many authors used heteroatom compounds to establish a series of indicators to define the levels of biodegradation of crude oil and investigate the origin of high acid crude oil [43–47]. For instance, Kim *et al.* (2005) observed a decrease of monocyclic O_2 species and an increase of di-, tri-, and tetracyclic O_2 species with increasing biodegradation levels, and the ratio of acyclic to 2–4 ring cyclic O_2-species were proposed to estimate the level of biodegradation [46].

However, above reported indicators are restricted to solely characterize either maturity or biodegradation degree of crude oil. Less work has been done on the reaction mechanisms of molecular component with the increasing of maturity and biodegradation degree. In this study, we attempt to establish a new parameter to simultaneously determine the evolution of maturity and biodegradation, and further discuss the reaction processes of major NSO compounds in crude oil.

2. Samples and methods

2.1. Oil samples

A total of 17 oil samples were collected from the Lower Cretaceous in major oilfields of the northern slope in the Bongor Basin, Chad in the northwest of Central African Shear Zone (Fig. S1). Table S1 shows the sample location and physical properties of the crude oils. Eight of the 17 samples within the suite with different biodegradation degrees have been described in Wang et al. (2023) [48]. The maturity of all oil samples has been calculated by Ts/(Ts + Tm) (Ts: C_{27} 18α-trisnorhopane; Tm: C_{27} 17α-trisnorhopane) detected by GC–MS (Table S1) due to a minor influence of biodegradation on the ratio [7].

2.2. GC–MS

The results presented in this study are based on geochemical parameters calculated from the saturated and aromatic fractions of crude oils obtained by GC–MS. The GC–MS analyses of the saturated fractions were carried out on a 5975A instrument, equipped with an HP-5MS chromatographic column (60 m length, 0.25 mm inner diameter, and 0.25 μm film thickness). Helium (purity > 99.999 %) was used as the carrier gas. The oven temperature was initially set at 50 ℃, with a one-minute hold. It was then raised to 120 ℃ at 20 ℃/min during the first stage, and then to 310 ℃ at 3 ℃/min during the second stage, where it was held for 20 mins. Electron impact ionization (70 eV) was employed.

The GC–MS analyses of the aromatic fractions were carried out using a 5977A instrument, equipped with an HP-5MS chromatographic column (60 m length, 0.25 mm inner diameter, and 0.25 μm film thickness). Helium (purity > 99.999 %) was used as the carrier gas. The initial oven temperature was set at 80 ℃, held for one minute and then raised to 310 ℃ at 3 ℃/min, where it was held for 20 mins. The mass spectrometer was operated in full scan, electron impact mode with electron energy of 70 eV.

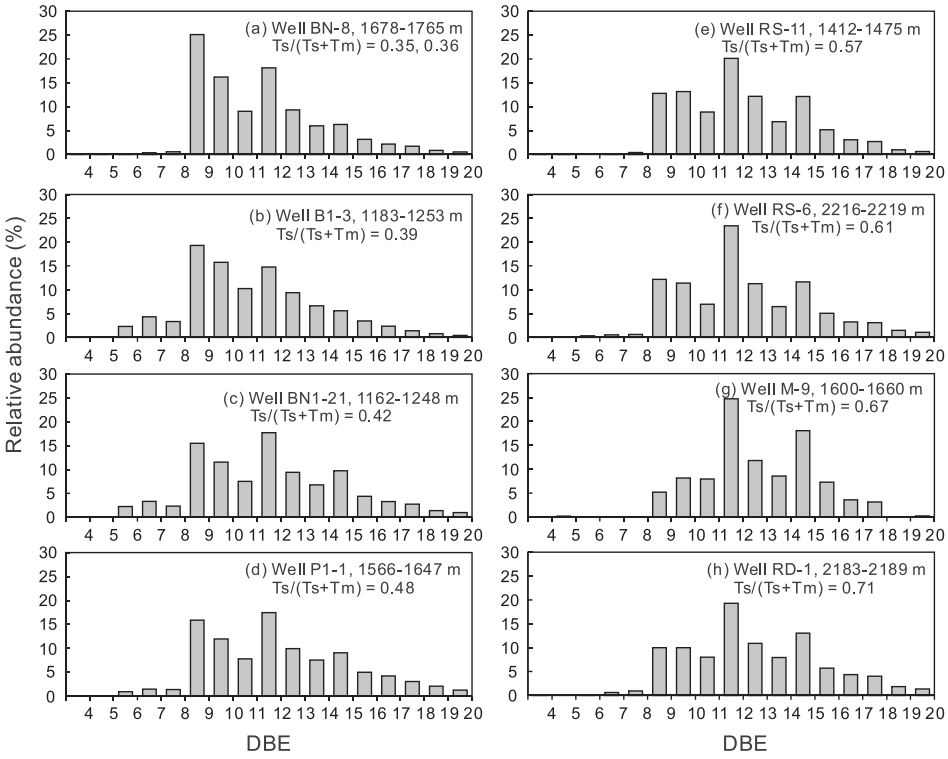

Fig. 1. The DBE value distributions of N_1 species from crude oil samples with different maturity. a–b: oils with low maturity; c–f: oils with moderate maturity; g–h: oils with high maturity.

2.3. (-) ESI FT ICR MS

About 10 mg of each oil sample was thoroughly dissolved using 1 mL of distilling toluene to prepare the mother solution with 10 mg/mL. Samples were prepared by dissolving 20 μL of the mother solution in 1 mL of toluene/methanol (1:3 v/v). About 1 μL of ammonium hydroxide solution was injected to facilitate deprotonation of the nitrogen- and oxygen-containing compounds prior to the FT ICR MS analysis. The high-resolution mass spectrometry analysis of the oil samples was conducted on a Bruker Apex-Ultra FT ICR mass spectrometer (made by Bruker Daltonic Inc., USA) equipped with a 9.4 T superconducting magnet. Sample solutions were injected into an Apollo II electrospray source in the negative ion mode with a rate of 250 μL/h using a syringe pump. The experiment conditions and concrete methods are as follows: emitter voltage, 4.0 kV; capillary column introduce voltage, 4.5 kV; and capillary column end voltage, −320 V; ions accumulated time, 0.1 s; ions scanning range, 200–1000 Da. The main running parameters of this instrument during obtaining the results have been listed in Table S2. The average errors were less than 0.5 ppm and 1.0 ppm for the internal and external calibration methods respectively in the mass range of 100–1500 Da. The mass calibration and data analysis were detailly presented by Shi et al. (2010a) [49]. The compounds ranging in *m/z* 200–1000 Da with greater than five times the standard deviation of the baseline noise in relative abundance were exported to a spreadsheet [49]. And then data analysis was carried out by selecting a two-mass scale-expanded segment near the most abundant compounds of the mass spectrum, followed by detailed identification of each compound. The major heteroatomic compounds were classified based on their elemental composition and double bond equivalent (DBE). The DBE, representing the degree of unsaturation (or hydrogen deficiency), contains aromatic rings as well as double bonds (with at least one carbon (C) atom). For a given compound ($C_cH_hN_nO_oS_s$), the DBE can be calculated from DBE = c − 0.5 h + 0.5n + 1, and the number of oxygen and sulfur atoms is not included in this formula. The acceptable mass error was set to ± 1 ppm for singly-charged ions. The average errors in formula assignment of the major compounds in the study are listed in Table S3.

3. Results

3.1. Variations in N_1 species during maturation

The DBE distributions of N_1 species considerably varies with ongoing maturation of crude oils (Fig. 1). The crude oils with low maturities from well BN-8 have a bimodal distribution pattern with DBE = 9 and DBE = 12 and maximal relative content of 25 % and 18 %, respectively (Fig. 1a, b). In the oil samples of moderate maturity, the relative abundance of DBE = 9 decreases and that of DBE = 12 and DBE = 15 increase with the increasing of oil maturity (Fig. 1c-f). And the DBE = 12 of N_1 species is preponderant in crude oils of moderate maturity (Fig. 1b-f). In the selected oil samples of wells M9 and RD-1 with the late oil window, those oils show a bimodal distribution pattern with DBE = 12 and DBE = 15 (Fig. 1g-h). The content of the value of DBE = 15 of N_1 species in high mature oils are higher than that of moderately mature oils (Table S3).

As an illustration, the characterization of carbon number distributions of N_1 species of oil samples at the various maturity stages is detailly presented for the carbon number distributions of the value of DBE = 12 of N_1 series compounds. The maximal relative intensities of carbon number are C_{20} in all oil samples and the peak intensity tends to increase with increasing maturity (Fig. S2). The carbon numbers of N_1 species with DBE = 12 of oils within the low and moderate maturity stages range from C_{17} to C_{52}, but the content of C_{35}-C_{52} compounds significantly decreases with increasing maturity (Fig. S2a-f). However, for oil samples with high maturity from wells M9 and RD-1, N_1-containing compounds with carbon numbers ranging in 17–38 are observed indicating a very steep drop in the content of carbazoles with alkyl side chains (Fig. S2h).

3.2. Variations in N_1 species during biodegradation

A modified van Krevelen plot provides a useful graphical exhibit to

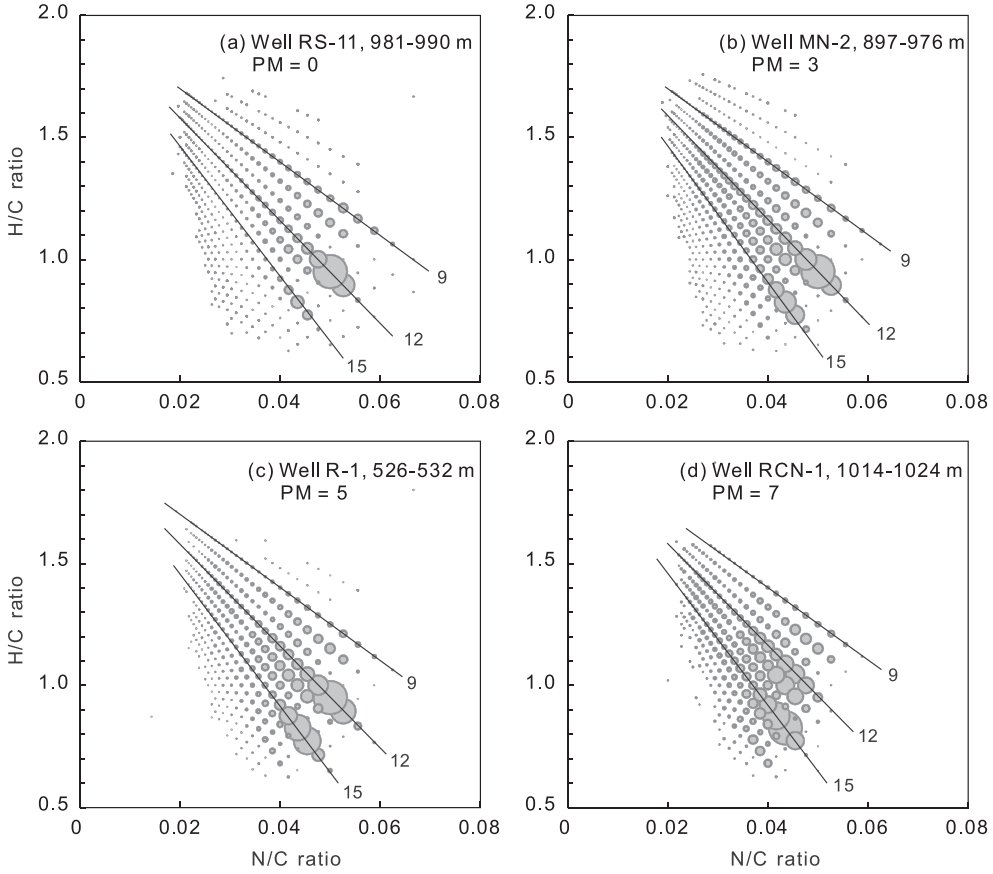

Fig. 2. 3D van Krevelen diagram of nitrogen-containing compounds identified in crude oils of different biodegradation levels. a: non-biodegraded; b: moderate biodegradation; c: heavy biodegradation; d: severe biodegradation. The bubble size shows the relative abundance of N_1 species with different DBE values and carbon numbers.

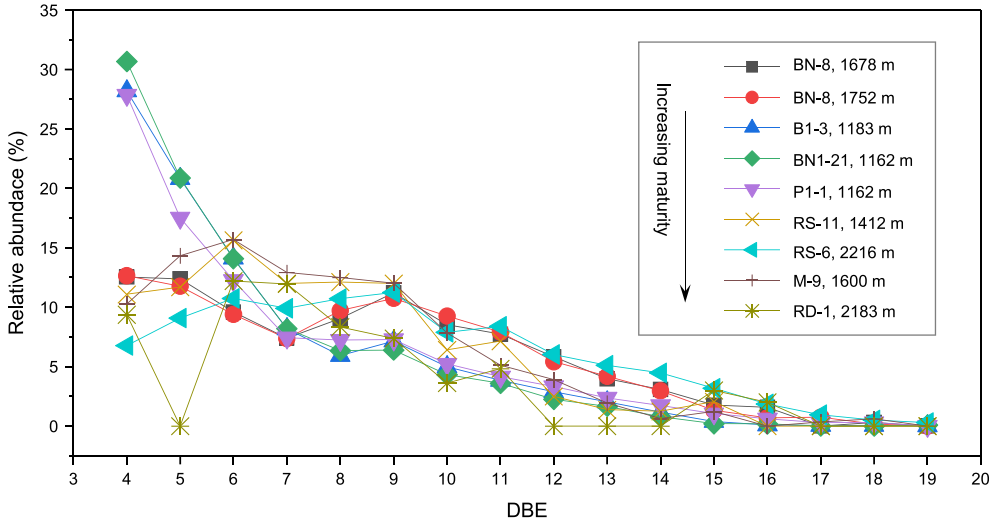

Fig. 3. Distribution of DBE of O_1 species of crude oil of different maturities.

investigate and analyze complicated mass spectra. Fig. 2 illustrates the modified 3D van Krevelen plots to show the major nitrogen-containing compounds (N_1 species) in collected crude oil samples with different biodegradation degrees. The variations of the number of hydrogen and nitrogen atoms relative to carbon atoms in the monoisotopic assigned peaks of N_1 species are expressed as the N/C ratio (x-axis) and H/C ratio (y-axis). and their relative abundance is presented by the bubble size. Changes in the N/C ratio are ascribed the number of carbon atoms in the compounds due to the constant of the number of nitrogen atoms in N_1 species. Values of the ordinate show the variation of hydrogen atoms and can be indicative of the degree of saturation as well as aromaticity of compounds. The modified van Krevelen plots indicate distinct variations in the DBE distributions of the N_1-classes with ongoing biodegradation (Fig. 2). Carbazoles (DBE = 9) and benzocarbazoles (DBE = 12) are predominate in the non-degraded (Fig. 2a) and mildly biodegraded oils (Fig. 2b), but dibenzocarbazoles (DBE = 15) sharply enhance with

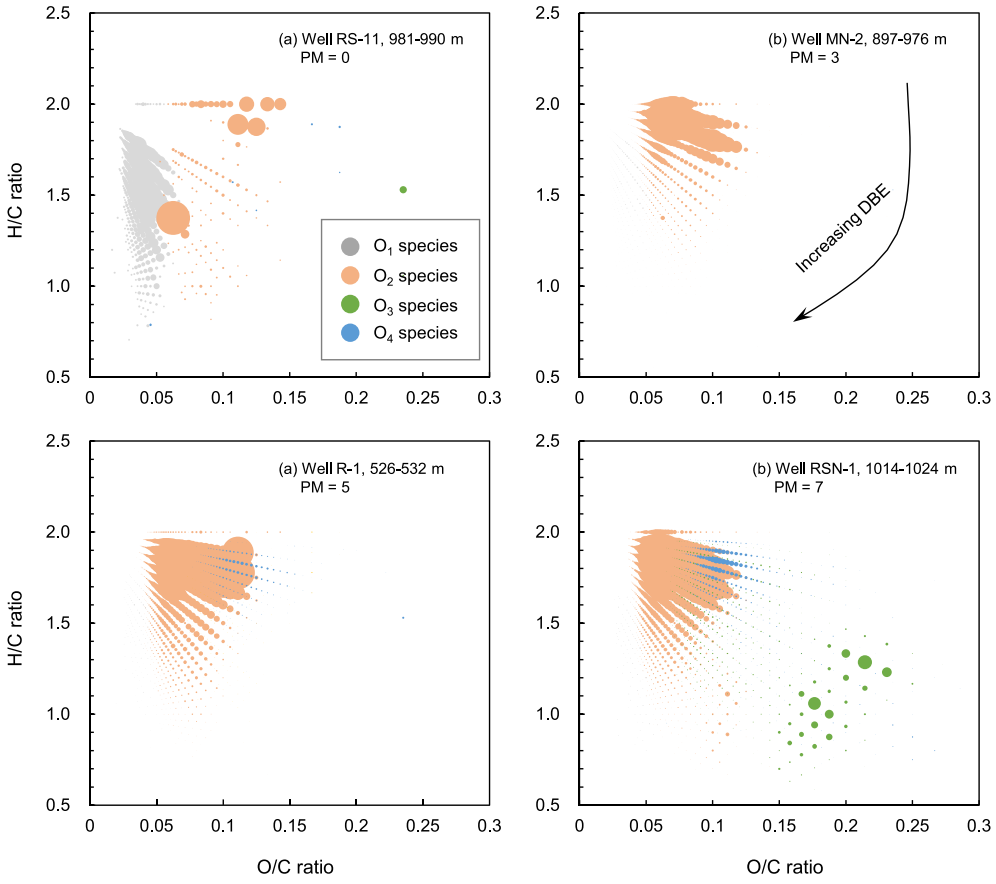

Fig. 4. 3D van Krevelen diagram of oxygen-containing compounds identified in crude oils of different biodegradation levels. a: non-biodegraded; b: moderate biodegradation; c: heavy biodegradation; d: severe biodegradation.

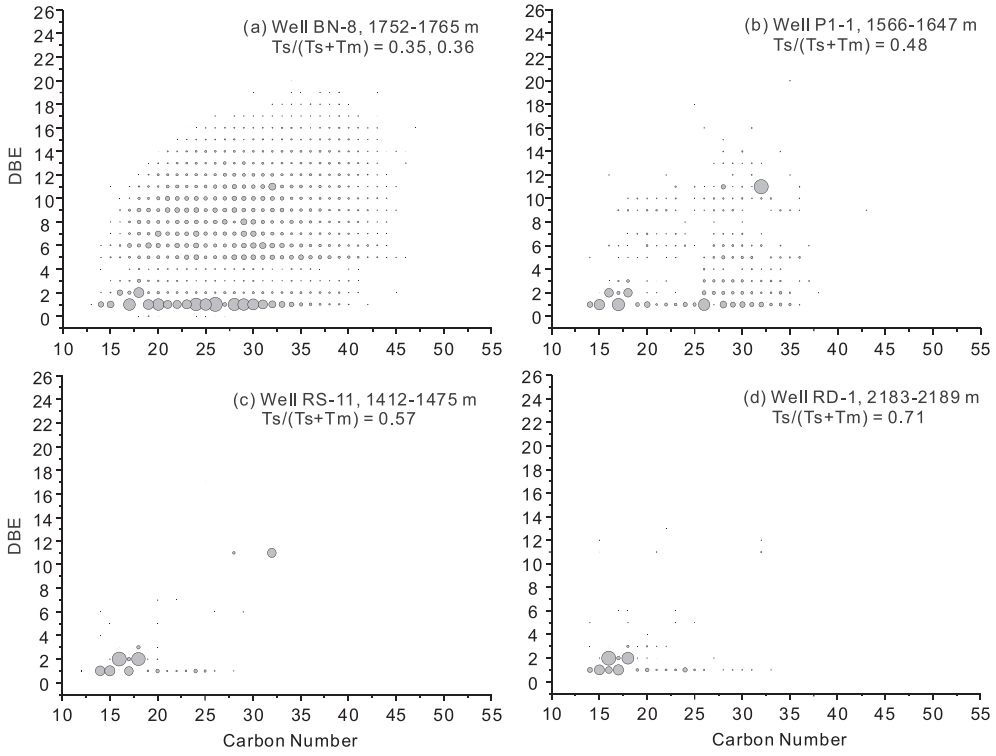

Fig. 5. Relative abundances of O_2 species as a function of DBE and carbon number in crude oils of different maturity. a: low maturity; b: moderate maturity; c-d: high matrity.

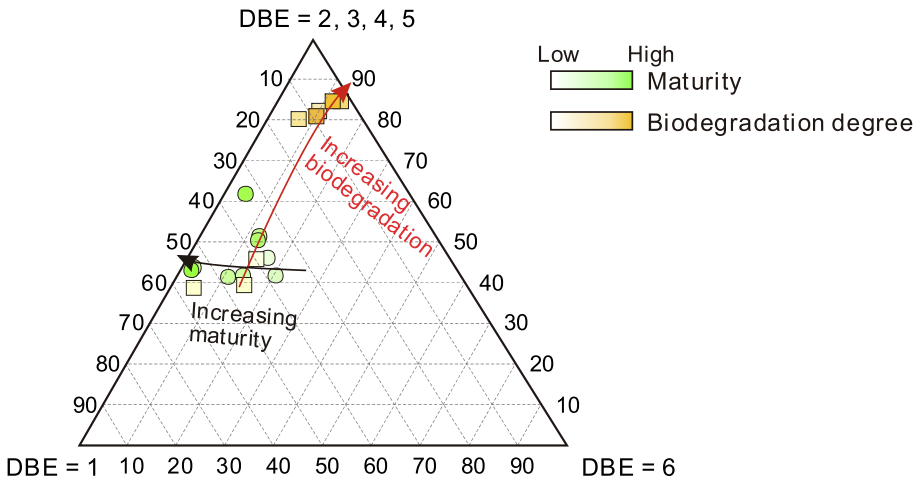

Fig. 6. Ternary diagram showing the effect of maturity and biodegradation degree changes of crude oils on the relative abundance of DBE = 1, DBE = 2, 3, 4, 5 and DBE = 6 of O_2 species.

increasing biodegradation degree and are dominated in severely degraded (Fig. 2c) and very severely degraded oils (Fig. 2d).

3.3. Variations in O_1 species during maturation

The DBE distributions of O_1 species in oils with different maturities are shown in Fig. 3. The enrichment of O_1-containing compounds in crude oil likely represents aromatic alcohols or fully aromatized compounds such as phenols, rather than aldehydes. The maximal mass peaks of DBE of O_1 species tend to shift to higher DBEs with the increasing of maturity. The DBE values of oil sample with lower-moderate maturity begin and maximize at 4, and the relative content gradually declines with advancing DBE value and is depleted in 16. The O_1 species in crude oils with high maturity start at DBE = 4 and bear a local maxima for higher DBE value range from 6 to 9 compared to lower-moderate mature oils (Fig. 3). The decrease in phenolic and/or benzylic O-species is attributed to alkylation and aromatization with increasing maturity.

3.4. Variations in O_1 species during biodegradation

The modified van Krevelen plots shown in Fig. 4 clearly display the distributions of major oxygen-containing compounds (O_1, O_2 and O_{3+} species) in crude oil samples with different biodegradation levels. The relative content of O_1 species decrease to a low level in the severely degraded oils (PM = 5–7) (Fig. 4c, d). The content of O_{3+} species is observed at a low level in oil samples of PM = 0 and PM = 3 (Fig. 4a, b) and increase as biodegradation proceed. The distribution of O_2 species obviously changes based on DBE value and degree of alkylation. Acyclic acids (DBE = 1) occur at a high level in non-biodegraded oils (Fig. 4a, b) and are gradually consumed with increasing biodegradation degree (Fig. 4c) and eliminated completely in the most severely degraded samples (Fig. 4d). The relative contents of DBE = 2, 3 and 4 of O_2 species increase with increasing biodegradation level and likely refer to partial oxidation of mono-, di-, and tri-cyclic saturated hydrocarbons. O_2 species with DBE = 5 bear analogous change, but perhaps indeterminate as those compounds correspond to a composite of carboxylated tetracyclic naphthenes and tetralins [46].

3.5. Variations in O_2 species during maturation

Fig. 5 illustrates the relative content of O_2 species for the distribution of carbon number versus the distribution of DBE. The O_2-containing compound distributions in oils significantly change as different maturities. The O_2 species is only abundant in the low mature oils (Fig. 5a, b) and becomes depleted with increasing thermal maturation stage (Fig. 5c, d), most likely attributable to unremitting decarboxylation. Such variation is intended, consisting with the noted tendencies of different compounds in the prior literature on oil and source rock [7,37].

3.6. Variations in O2 species during biodegradation

The changes in abundances of O_2 species with DBE ranging from 1 to 6 are illustrated by a ternary diagram (Fig. 6). Three end members on the modified triangle diagram are fatty acids (DBE = 1), naphthenic acids (DBE = 2, 3, 4, 5) and hopanoic acids (DBE = 6), respectively. It shows that the content of DBE = 6 of O_2 species sharply decrease with increasing maturity (Fig. 6).

3.7. Variations in major compound species during maturation

To reveal the comprehensive changes among different types of major compounds of crude oil with different maturities and biodegradation degrees, the relative content of each type of compound is summarized and displayed using two bar charts (Fig. S3). The content of N_1 species shows a distinct rising tendency with the increasing of maturity (Table S4). However, with ongoing increase in maturity, the change on the content of N_1O_x (i.e. N_1O_1, N_1O_2 and N_1O_3) species almost exactly opposite that of N_1 species. The proportion of O_1 species bears a distinct rising tendency at low–moderate mature oils and then decreases with the incremental maturity. Similar change trendy was observed in products of pyrolysis experiments of immature mudstone with organic-rich matter [37]. The relative percentages of O_2, O_3 and O_4 species overall decline with increasing maturity, and O_3 and O_4 species are little in high mature oils (Fig. S3a).

3.8. Variations in major compound species during biodegradation

The relative abundances of the 11 main components (i.e. N_y, N_yO_x, O_x, N_yS_z and O_xS_z) of the selected oil samples with various biodegradation degrees are presented in Fig S3 to visually examine the variations of those compounds. The most abundant compounds in non-biodegraded (PM = 0) and lightly biodegraded (PM = 1) oils are N_1 species. The share of the N_1 species is over 70 %. The O_1 species are enriched in oil samples with PM = 0, PM = 1 and PM = 2, and an intuitive decrease of their relative abundance occur in severe biodegraded oils (Fig. S3b). However, O_2, O_3 and O_4 containing compounds become dominated in highly biodegraded oils, and they form above 80 % of the total abundances.

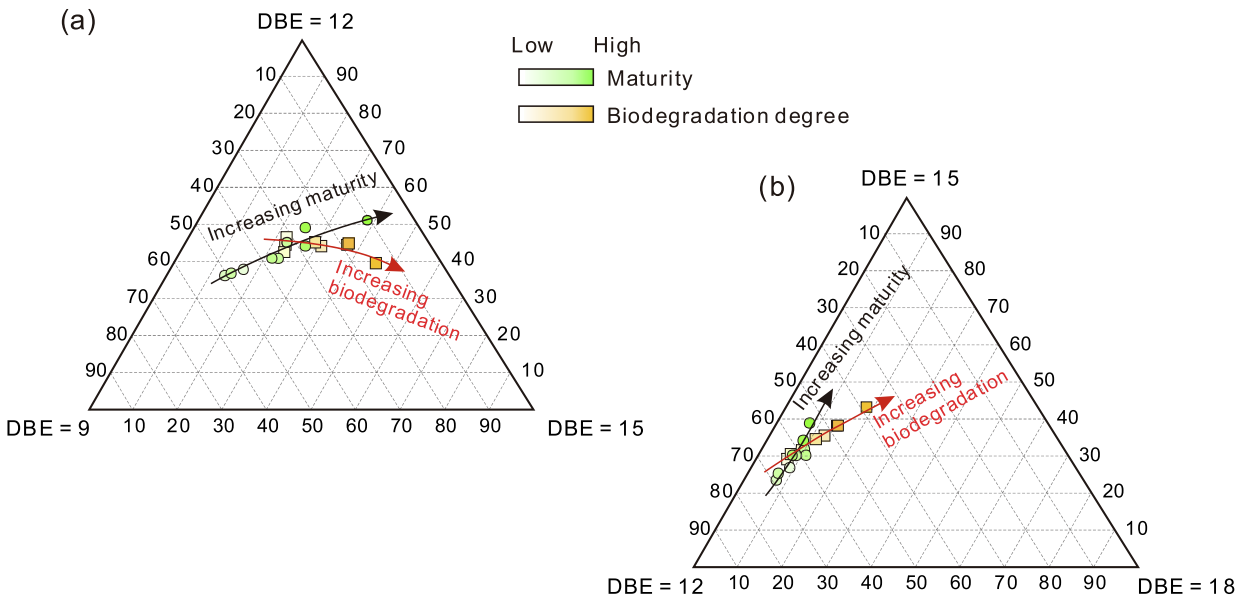

Fig. 7. Ternary diagrams showing the effect of maturity and biodegradation degree changes of crude oils on the relative abundance of (a) DBE = 9, DBE = 12, DBE = 15 and (b) DBE = 12, DBE = 15, DBE = 18 of N_1 species.

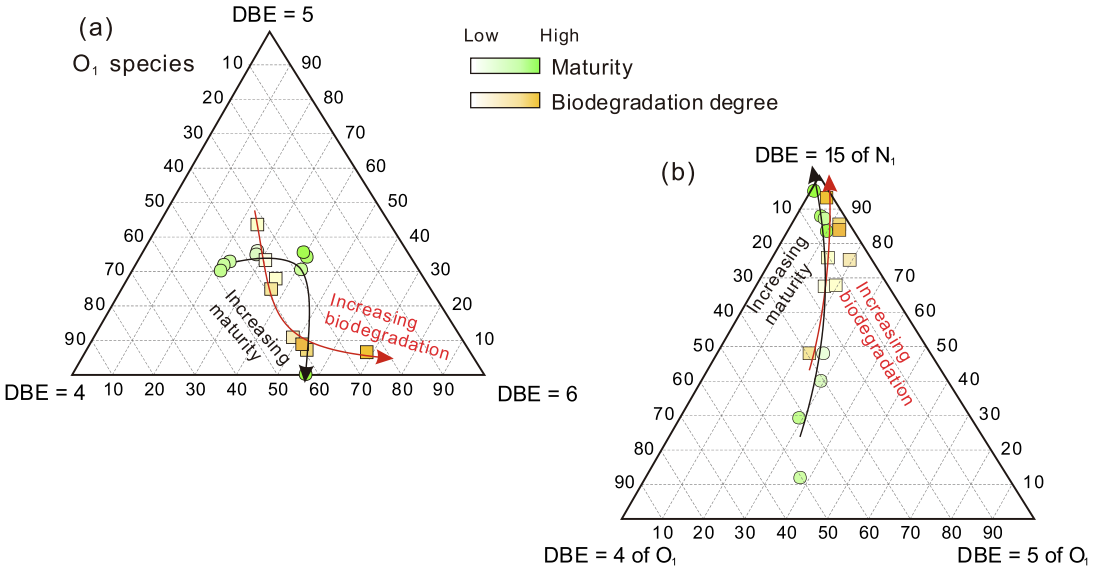

Fig. 8. Ternary diagram showing the effect of maturity and biodegradation degree changes of crude oils on (a) the relative abundance of DBE = 4, DBE = 5 and DBE = 6 of O_1 species; (b) the relative abundance of DBE = 4 and DBE = 5 of O_1 species and DBE = 15 of N_1 species.

4. Disscussion

4.1. Effects of maturity on changes in NSO compounds

4.1.1. N_1 Species

Different DBE components of N_1 species are widely applied to assess maturity of crude oil and source rock. The relative content of carbazole (DBE = 9) decreases and that of benzocarbazole (DBE = 12) and dibenzocarbazole (DBE = 15) increases with increasing maturity (Fig. 7a), which may be due to continuous condensation by small molecule and result in high condensation degree species increasingly dominated in relative abundance [33–35]. Similar changes also occur in the ternary diagram including DBE = 12, DBE = 15 and DBE = 18 of N_1 species (Fig. 7b).

4.1.2. O_1 species

The distributions of O_1 species is affected by maturation processes. The low to moderate mature oils have relatively abundant DBE = 5 compounds (Fig. 8a). Therefore, with increasing maturity, the O_1 species is increasingly dominated in relative content by the more aromatized compounds.

Ziegs et al. (2018) provided a ternary diagram including phenolic species (O_1 species with DBE = 4 and 5) and dibenzocarbazoles (N_1 species with DBE = 15) for maturity assessment, which is applied to both carbonate reservoir and siliciclastic reservoir [39]. Fig. 8b shows the relative abundance of N_1 species with DBE = 15 and O_1 species with DBE = 4 and 5. The results indicate that data points with high maturity tend to shift to dibenzocarbazoles (DBE = 15, N_1 species) end-member, suggesting that lower mature oils bear more abundance in O_1 species with DBE = 4 and 5 than high mature oils, caused by alkylation and aromatization as maturity proceed.

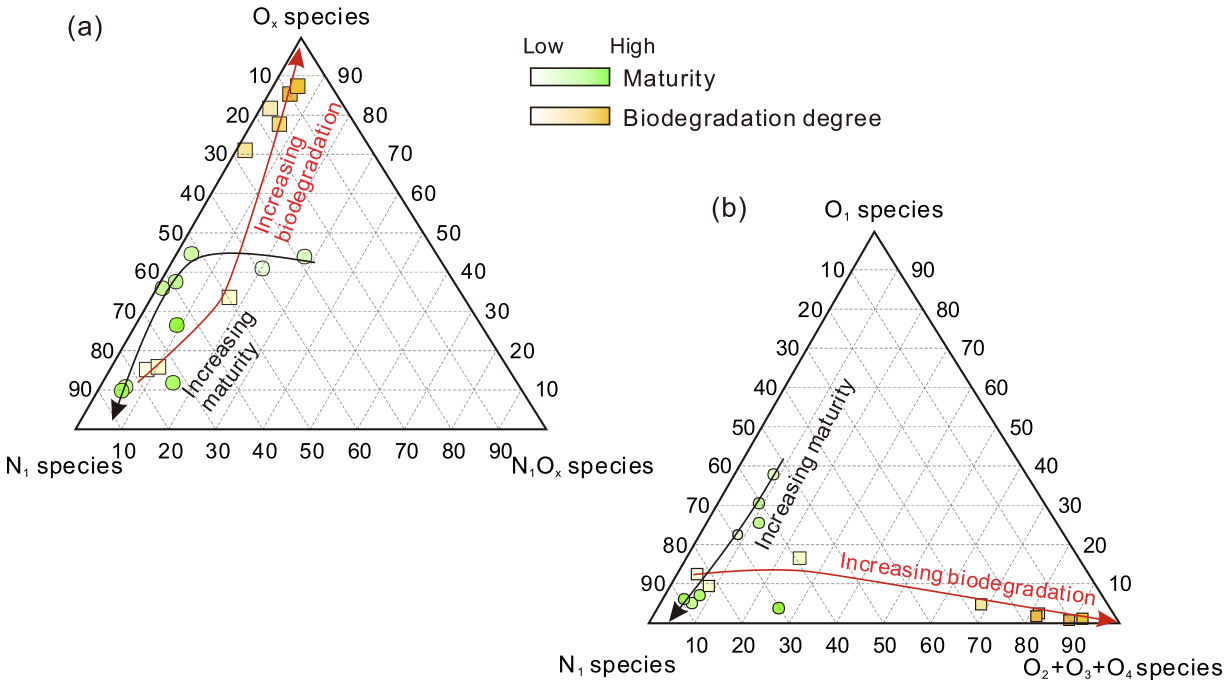

Fig. 9. Ternary diagram showing the effect of maturity and biodegradation degree changes of crude oils on (a) the relative abundance of N_1, O_x and N_1O_x species; (b) the relative abundance of N_1, O_1 and $O_2 + O_3 + O_4$ species.

4.1.3. O_2 species

Fig. 5 shows a decrease tendency of O_2 during maturation. The cause of the decreased is probably that oxygen atoms combined with nitrogen and carbon are released as relatively non-active low molecular weight compounds (e.g. CO_2, H_2O, NH_3 and CH_4) with ongoing maturation. The DBE value of the most abundance of O_2 species displays a sharp decline of naphthenic acids (DBE = 3, 4), aromatic carboxylic acids and diols (compounds with DBE values > 5). The variations in the distribution of carbon number of all DBE classes are the decreased degree of alkylation due to side chain cracking reactions. The appellation of the DBE = 6 mainly to hopanoic acids is confirmed by reported correspondences to the abundance of hopanoic acids with increasing microbial alteration [46]. C_{30}-C_{32} hopanoic acids are abundant in low mature crude oils. However, the content of hopanoic acids become less as maturity becomes higher. The hopanoic acids are being generated by some specific bacteria bacteria, i.e. degrading bacteria. It is speculated that the various changes in the distributions of hopanoic acid mirror changes in microbial population as maturity proceeds.

4.2. Effects of biodegradation on changes in NSO compounds

4.2.1. N_1 Species

For oil samples with different biodegradation levels, all samples fall into a straight line in the ternary diagram and datapoint of severely biodegraded oils tends to shift to DBE = 15 end-member (Fig. 7a) due to a comparatively stronger decline of DBE = 9 and DBE = 12 compounds, indicating small molecule continuous consumed by microorganisms and converted into macromolecule. In the ternary diagram of the benzocarbazoles, dibenzocarbazoles and benzonaphthocarbazoles (DBE = 18), the samples distribute on a straight line and occur a downtrend of benzocarbazoles with increasing biodegradation degree (Fig. 7b), which is consist with the decrease of N/C ratios (Fig. 2).

4.2.2. O_1 species

Biodegradation is sensitive to the distribution of O_1 species. Fig. 8a displays an evident relative content of the higher benzannulated homologues (DBE = 6) increase with increasing biodegradation degree. The non-biodegraded and lightly biodegraded oils contain the relatively abundant DBE = 4 and DBE = 5 classes. The content of those compounds decreases with increasing biodegradation level due to aromatization [47]. The oil samples with severe biodegradation bears the highest amounts of DBE = 6 (Fig. 8a).

Similar tendency occurs in crude oils with increasing biodegradation level (Fig. 8b). O_1 species are more enriched in oils with low biodegradation degree (Fig. 4a) and slowly depleted with increasing biodegradation degree, resulting from a preferential consumption of O_1 species as biodegradation proceed.

4.2.3. O_2 species

It shows that the content of DBE = 6 of O_2 species sharply decrease with increasing maturity (Fig. 6). This shift in hopanoic acid distribution shows that different microbial populations, possibly consisting of archaea or non-hopanoid-producing bacteria, become primary under such conditions. However, the peak to severely biodegraded oils shows a relative enrichment of DBE = 2–5 over 80 % (Fig. 6). The variation is most likely due to the generation of naphthenic acids by demethylation and cyclization reactions by removal of fatty acids during biodegradation [47]. The relative content of DBE = 6 class is relatively invariant, which may be attributed to unchanged microbial population in the course of oil alteration.

To sum up, oil datasets of different maturities and biodegradation degrees overall show similar features in the ternary diagram of DBE = 9, DBE = 12 and DBE = 15 and the ternary diagram of DBE = 12, DBE = 15 and DBE = 18 of N_1 species, as well as the ternary diagram composed of O_1 and O_2-containing compounds.

4.3. New maturity and biodegradation degree parameters

With the increasing of maturity and biodegradation degree, the relative contents of N_1 species with DBE = 9 and that of DBE = 12 both decrease in the ternary diagram of DBE = 9, DBE = 12 and DBE = 15 and the ternary diagram of DBE = 12, DBE = 15 and DBE = 18, respectively (Fig. 2). The relative abundance of O_1 species with DBE = 4 both decreases and that of N_1 species with DBE = 15 both increases of oil

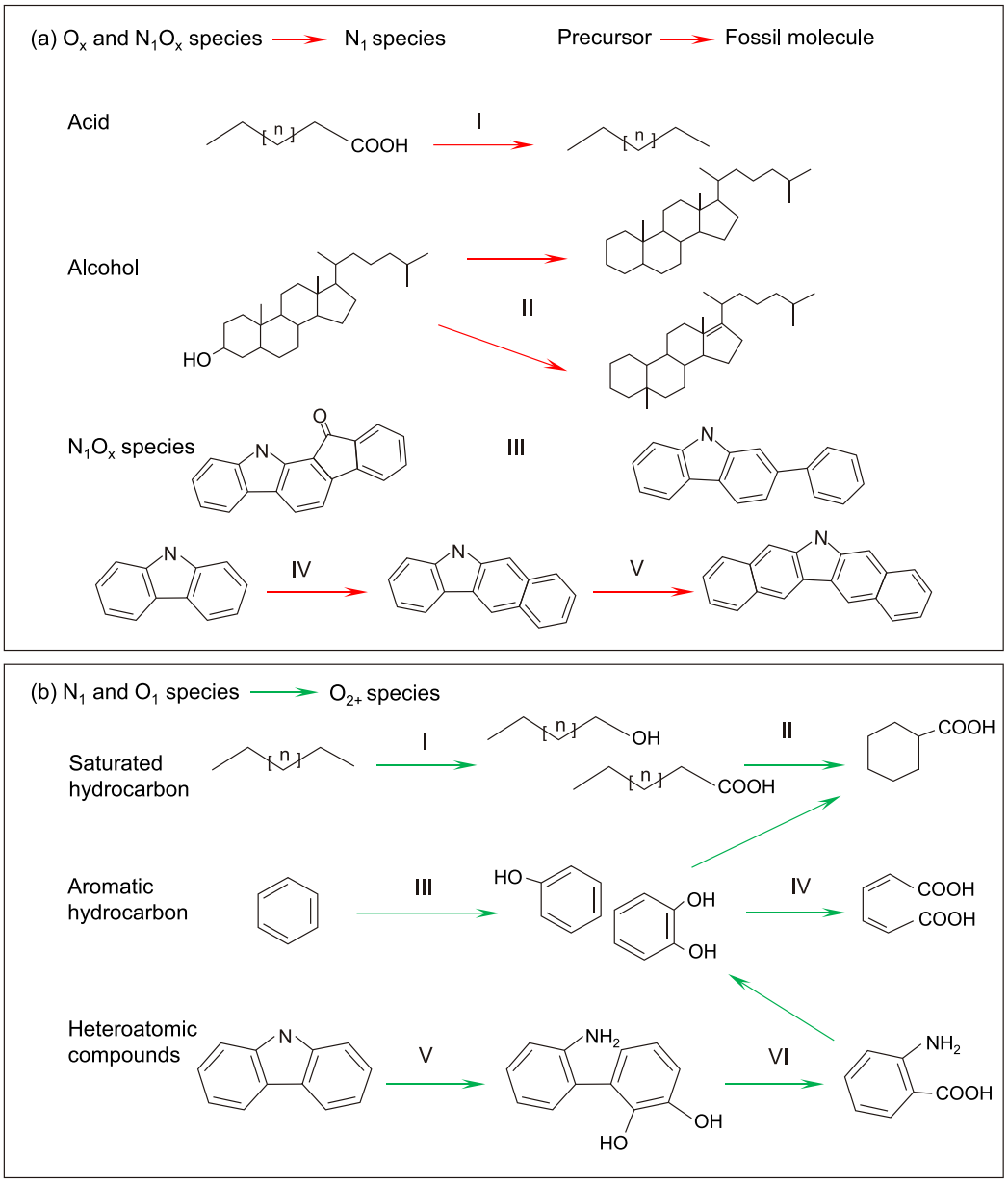

Fig. 10. Schematic transformation and formation pathways for major heteroatomic compounds of crude oil during (a) maturation and (b) biodegradation.

samples in the ternary diagram of DBE = 4, DBE = 5 and DBE = 6 of O_1 species and the ternary diagram of DBE = 4 of O_1 species, DBE = 5 of O_1 species and DBE = 15 of N_1 species, respectively (Fig. 5) as increased maturity and biodegradation degree. The components of O_2 species with DBE = 1–6 of oils with the increasing of maturity and biodegradation level both are no distinct rule in the ternary diagram of DBE = 1, DBE = 2, 3, 4, 5 and DBE = 6 of O_2 species (Fig. 8). Therefore, the indicators reported by previous authors may be not useful for maturity assessment when the oil undergo secondary alteration such as biodegradation. However, in this paper, the changes on relative content of N_1 species and that of O_2 species of oil samples are very different with the increasing of maturity and biodegradation degree (Figure S3).

The relative component of N_1, O_x and N_1O_x species of crude oils with different maturities and biodegradation degrees is shown in Fig. 9a. The relative content of N_1O_x species bears the changes of decrease when Ts/Tm < 0.42 and then almost invariability with increasing maturity. Nevertheless, the relative content of O_x species gradually declines as ongoing maturity. Oil samples with high maturity have higher contents of N_1 species (Fig. 9a). This change is consistent with the results of a pyrolysis experiment of immature source rock reported by Liang et al. (2023) [32]. However, in comparison with the evolution of maturation, oils with different biodegradation levels display different regularity changes in the ternary diagram. With increasing biodegradation levels, data points of severely biodegraded oils tend to shift to O_x species end-member (Fig. 9a).

The distribution of O_x species (O_1, O_2, O_3 and O_4 species) of oil samples with increasing maturity and biodegradation degree presents distinctly different changing trends (Fig. S2). Hence, a modified ternary diagram of N_1 species, O_1 species and $O_2 + O_3 + O_4$ species is used for defining the evolution of the component of crude oil during maturity and biodegradation process (Fig. 9b). The results show that the relative content of O_1 species in oils decreases with increasing maturity. Oil samples with high maturity are characterized by high content of N_1 species. Whereas, with increasing biodegradation degree, the relative content of N_1 species decline and that of $O_2 + O_3 + O_4$ species obviously increase (Fig. 9b).

4.4. Reaction pathways of compound species during maturation and biodegradation

4.4.1. Maturation processes

The results above demonstrate that major compositional variations are different in the acidic and neutral compounds of the crude oil with ongoing maturation and biodegradation (Fig. 8; Fig. 9; Fig. S2), which reflects different mechanisms of generation, transformation, and expulsion of organic compounds. Acids and alcohols generated from living organisms are abundant in crude oil in the low mature stage [50] (Fig. 4; Fig. 7a, b; Fig. S2a). Then, with the increasing of maturity, these compounds are converted to alkanes by the loss of functional groups, stabilization of the molecule by hydrogenation, aromatization [6] (Fig. 10a I-II), which leads to a sharp decrease of O_1 and O_2-containing compounds (Fig. 4; Fig. 7c, d; Fig. S2a). The gradual decrease of N_1O_x species content in crude oil (Fig. S2a; Fig. 9a) may be attribute to the decarbonylation of keto group-containing compounds during maturation [34], which enhance the formation of N_1 species (Fig. 7a; Fig. 9a; Fig. 10a III). Carbazole (DBE = 9) likely transform into benzocarbazole (DBE = 12) and then convert to dibenzocarbazole (DBE = 15) by demethylation and aromatization with increasing maturation stage [39] (Fig. 10a V-VI). This reaction process can interpret the increase of DBE of N_1 species (Fig. 3) and a decrease of carbon number range of each DBE class and a shift to lower carbon numbers (Fig. 1; Fig. 2).

4.4.2. Biodegradation processes

The normal alkanes primarily are consumed [13,51] and converted to fatty alcohols and then reduced into fatty acids (Fig. 10b I). Therefore, fatty acids are abundant in slightly biodegraded oils (Fig. 5a, b; Fig. 8a). The fatty acids present cyclization reactions to form naphthenic acids with increasing biodegradation [46,52–54] (Fig. 10b II). As biodegradation steadily proceed, aromatic compounds and heteroatomic compounds are consistently altered and transformed into naphthenic acids and O_4 species containing two hydroxyl groups (Fig. 5c, d; Fig. 10b III-IV). N_1-containing compounds are biodegraded by ring-opening reaction and converted into N_1O_x species in the stage of severe biodegradation [55–58] (Fig. 10b V-VI). Those N_1O_x compounds is gradually oxidized to alcohols and acids by microorganism [58]. These reactions are confirmed by the consistent decline in N_1 species and first increase and then decrease in N_1O_x species (Fig. 9a; Fig. S2b).

5. Conclusion

In this paper, the nitrogen- and oxygen-containing compounds in crude oils with different maturities and biodegradation degrees have been characterized by ESI FT-ICR MS. Based on the distinct changes of molecule components with increasing maturity and biodegradation degree, a new ternary diagram composed of three end-numbers of N_1, O_1 and $O_2 + O_3 + O_4$ species, respectively is proposed. Datasets of the oils with maturity increased gradually shift to N_1 species end-member and turn away from O_1 and $O_2 + O_3 + O_4$ species end-members indicating an increasing of N_1 compounds and a decreasing of O_1 and O_2 compounds, which may be due to decarboxylation and dehydration. However, Data points of the oils as biodegradation proceed shift to $O_2 + O_3 + O_4$ species end-member and are away from N_1 species end-member showing a decreasing of N_1 compounds and an increasing of $O_2 + O_3 + O_4$ compounds because of microbiological alteration and oxidization. Therefore, the ternary diagram of N_1, O_1 and $O_2 + O_3 + O_4$ species is a useful method to jointly assess the degrees of maturity and biodegradation of crude oil.

CRediT authorship contribution statement

Dongyong Wang: Writing – original draft, Resources, Formal analysis, Data curation, Conceptualization. **Meijun Li:** . **Jianfa Chen:** Writing – review & editing, Resources, Methodology, Investigation, Formal analysis. **Haochen Chen:** Writing – original draft, Visualization, Software, Methodology, Investigation. **Quan Shi:** Writing – review & editing, Resources, Methodology, Investigation.

Declaration of competing interest

The authors declare that they have no known competing financial interests or personal relationships that could have appeared to influence the work reported in this paper.

Data availability

Data will be made available on request.

Acknowledgements

The work was funded by the National Natural Science Foundation of China (Grant No. 41073054). The authors thank Dr. Kevin Van Geem and two anonymous reviewers for their constructive suggestions. Thanks to the Research Institute of Petroleum Exploration and Development, PetroChina for providing oil samples and permission to publish.

Appendix A. Supplementary data

Supplementary data to this article can be found online at https://doi.org/10.1016/j.fuel.2023.130499.

References

[1] Radke M, Welte DH, Willsch H. Geochemical study on a well in the Western Canada Basin: relation of the aromatic distribution pattern to maturity of organic matter. Geochim Cosmochim Acta 1982;46:1–10.
[2] Alexander R, Kagi RI, Rowland SJ, Sheppard PN, Chirila TV. The effects of thermal maturity on distributions of dimethylnaphthalenes and trimethylnaphthalenes in some Ancient sediments and petroleums. Geochim Cosmochim Acta 1985;49:385–95.
[3] Hunt JM. Petroleum geochemistry and geology. Second edition ed: WH Freeman Company 1995.
[4] Yang S, Li M, Liu X, Han Q, Wu J, Zhong N. Thermodynamic stability of methyldibenzothiophenes in sedimentary rock extracts: Based on molecular simulation and geochemical data. Org Geochem 2019;129:24–41.
[5] Li M, Zhong N, Shi S, Zhu L, Tang Y. The origin of trimethyldibenzothiophenes and their application as maturity indicators in sediments from the Liaohe Basin. East China Fuel 2013;103:299–307.
[6] Tissot BP, Welte DH. Petroleum Formation and Occurrence. Second. Edition ed. Heidelberg: Springer Verlag; 1984.
[7] Peters KE, Walters CC, Moldowan JM. The Biomarker Guide Volume 2: Biomarkers and Isotopes in Petroleum Systems and Earth History. Second Edition ed, Cambridge: Cambridge University Press; 2005.
[8] Wang D, Li M, Zhou Y, Yang L, Yang Y, Li E, et al. Petroleum geochemistry and origin of shallow-buried saline lacustrine oils in the slope zone of the Mahu sag, Junggar Basin, NW China. Pet Sci 2023.
[9] Xiao H, Li M, Liu J, Mao F, Cheng D, Yang Z. Oil-oil and oil-source rock correlations in the Muglad Basin, Sudan and South Sudan: New insights from molecular markers analyses. Mar Pet Geol 2019;103:351–65.
[10] Kvalheim OM, Christy AA, Telnaes N, Bjorseth A. Maturity determination of organic matter in coals using the methylphenanthrene distribution. Geochim Cosmochim Acta 1987;51:1883–8.
[11] Fang R, Wang TG, Li M, Xiao Z, Zhang B, Huang S, et al. Dibenzothiophenes and benzonaphthothiophenes: Molecular markers for tracing oil filling pathways in the carbonate reservoir of the Tarim Basin. NW China Org Geochem 2016;91:68–80.
[12] Huang H, Bowler BFJ, Oldenburg TBP, Larter SR. The effect of biodegradation on polycyclic aromatic hydrocarbons in reservoired oils from the Liaohe basin. NE China Org Geochem 2004;35:1619–34.
[13] Huang H, Yin M, Han D. Novel parameters derived from alkylchrysenes to differentiate severe biodegradation influence on molecular compositions in crude oils. Fuel 2020;268:117366.
[14] Larter SR, Huang H, Adams J, Bennett B, Jokanola O, Oldenburg T, et al. The controls on the composition of biodegraded oils in the deep subsurface; Part II, Geological controls on subsurface biodegradation fluxes and constraints on reservoir-fluid property prediction. AAPG Bull 2006;90:921–38.
[15] Baker EW, William Louda J, Orr WL. Application of metalloporphyrin biomarkers as petroleum maturity indicators: The importance of quantitation. Org Geochem 1987;11:303–9.
[16] Chen JH, Philp RP. Porphyrin distributions in crude oils from the Jianghan and Biyang basins. China Chem Geol 1991;91:139–51.

[17] Jumina J, Kurniawan YS, Siswanta D, Purwono B, Zulkarnain AK, Winarno A, et al. The Origin, Physicochemical Properties, and Removal Technology of Metallic Porphyrins from Crude Oils. Indones J Chem 2021;21:1023–38.
[18] Li M, Wang TG, Shi S, Zhu L, Fang R. Oil maturity assessment using maturity indicators based on methylated dibenzothiophenes. Pet Sci 2014;11:234–46.
[19] Li M, Cheng D, Pan X, Dou L, Hou D, Shi Q, et al. Characterization of petroleum acids using combined FT-IR, FT-ICR–MS and GC–MS: Implications for the origin of high acidity oils in the Muglad Basin. Sudan Org Geochem 2010;41:959–65.
[20] Corilo YE, Vaz BG, Simas RC, Lopes Nascimento HD, Klitzke CF, Pereira RCL, et al. Petroleomics by EASI(±) FT-ICR MS. Anal Chem 2010;82:3990–6.
[21] Hendrickson CL, Emmett MR. Electrospray ionization fourier transtorm ion cyclotron resonance mass spectrometry. Annu Rev Phys Chem 1999;50:517–36.
[22] Hertzog J, Carré V, Le Brech Y, Mackay CL, Dufour A, Mašek O, et al. Combination of electrospray ionization, atmospheric pressure photoionization and laser desorption ionization Fourier transform ion cyclotronic resonance mass spectrometry for the investigation of complex mixtures – Application to the petroleomic analysis of bio-oils. Anal Chim Acta 2017;969:26–34.
[23] Shi Q, Zhao S, Xu Z, Chung KH, Zhang Y, Xu C. Distribution of Acids and Neutral Nitrogen Compounds in a Chinese Crude Oil and Its Fractions: Characterized by Negative-Ion Electrospray Ionization Fourier Transform Ion Cyclotron Resonance Mass Spectrometry. Energy Fuels 2010;24:4005–11.
[24] Vanini G, Barra TA, Souza LM, Madeira NCL, Gomes AO, Romão W, et al. Characterization of nonvolatile polar compounds from Brazilian oils by electrospray ionization with FT-ICR MS and Orbitrap-MS. Fuel 2020;282:118790.
[25] Marshall AG, Rodgers RP. Petroleomics: The Next Grand Challenge for Chemical Analysis. Acc Chem Res 2004;37:53–9.
[26] Kim S, Rodgers RP, Truly MAG. "exact" mass: Elemental composition can be determined uniquely from molecular mass measurement at ~0.1mDa accuracy for molecules up to ~500Da. Int J Mass Spectrom 2006;251:260–5.
[27] Marshall AG, Rodgers RP. Petroleomics: chemistry of the underworld. Proc Natl Acad Sci U S A 2008;105:18090–5.
[28] Shi Q, Zhang Y, Xu C, Zhao S, Chung KH. Progress and prospect on petroleum analysis by Fourier transform ion cyclotron resonance mass spectrometry. Sci China Chem 2014;44:694–700.
[29] Marshall AG, Hendrickson CL, Jackson GS. Fourier transform ion cyclotron resonance mass spectrometry: A primer. Mass Spectrom Rev 1998;17:1–35.
[30] Palacio Lozano DC, Thomas MJ, Jones HE, Barrow MP. Petroleomics: Tools, Challenges, and Developments. Ann Rev Anal Chem 2020;13:405–30.
[31] Poetz S, Kuske S, Song Y, Jweda J, Michael E, Horsfield B. Using polar nitrogen-, sulphur- and oxygen-compound compositions from ultra-high resolution mass spectrometry for petroleum fluid assessment in the Eagle Ford Formation, Texas. Geol Soc Lond Spec Publ 2019;484:71–96.
[32] Liang T, Zhan Z, Wang G, Zou Y. Resin composition: An indicator of oil maturity as revealed by fourier transform ion cyclotron resonance mass spectrometry. Pet Sci 2023;20:769–75.
[33] Oldenburg TBP, Brown M, Bennett B, Larter SR. The impact of thermal maturity level on the composition of crude oils, assessed using ultra-high resolution mass spectrometry. Org Geochem 2014;75:151–68.
[34] Poetz S, Horsfield B, Wilkes H. Maturity-Driven Generation and Transformation of Acidic Compounds in the Organic-Rich Posidonia Shale as Revealed by Electrospray Ionization Fourier Transform Ion Cyclotron Resonance Mass Spectrometry. Energy Fuels 2014;28:4877–88.
[35] Wan Z, Li S, Pang X, Dong Y, Wang Z, Chen X, et al. Characteristics and geochemical significance of heteroatom compounds in terrestrial oils by negative-ion electrospray Fourier transform ion cyclotron resonance mass spectrometry. Org Geochem 2017;111:34–55.
[36] Wang Q, Hao F, Cao Z, Tian J. Heteroatom compounds in oils from the Shuntuoguole low uplift, Tarim Basin characterized by (+ESI) FT-ICR MS: Implications for ultra-deep petroleum charges and alteration. Mar Pet Geol 2021;134:105321.
[37] Yan G, Xu Y, Liu Y, He W, Chang X, Tang P. The evolution of acids and neutral nitrogen-containing compounds during pyrolysis experiments on immature mudstone. Mar Pet Geol 2020;115:104292.
[38] Zhang H, Li S. GC–MS and ESI FT-ICR MS characterization on two type crude oils from the Dongying depression. Fuel 2023;333:126408.
[39] Ziegs V, Noah M, Poetz S, Horsfield B, Hartwig A, Rinna J, et al. Unravelling maturity- and migration-related carbazole and phenol distributions in Central Graben crude oils. Mar Pet Geol 2018;94:114–30.
[40] Mao D, Weghe HVD, Lookman R, Vanermen G, Brucker ND, Diels L. Resolving the unresolved complex mixture in motor oils using high-performance liquid chromatography followed by comprehensive two-dimensional gas chromatography. Fuel 2009;88:312–8.
[41] Wenger LM, Davis CL, Isaksen GH. Multiple Controls on Petroleum Biodegradation and Impact on Oil Quality. SPE Reserv Eval Eng 2002;5:375–83.
[42] El-Sabagh SM. Occurrence and distribution of vanadyl porphyrins in Saudi Arabian crude oils. Fuel Process Technol 1998;57:65–78.
[43] Oldenburg TBP, Jones M, Huang H, Bennett B, Shafiee NS, Head I, et al. The controls on the composition of biodegraded oils in the deep subsurface – Part 4. Destruction and production of high molecular weight non-hydrocarbon species and destruction of aromatic hydrocarbons during progressive in-reservoir biodegradation. Org Geochem 2017;114:57–80.
[44] Meng Q, Wang X, Liao Y, Lei Y, Yin J, Liu P, et al. The effect of slight to moderate biodegradation on the shale soluble organic matter composition of the upper triassic Yanchang formation, Ordos Basin. China Mar Pet Geol 2021;128:105021.
[45] Liu W, Liao Y, Pan Y, Jiang B, Zeng Q, Shi Q, et al. Use of ESI FT–ICR MS to investigate molecular transformation in simulated aerobic biodegradation of a sulfur-rich crude oil. Org Geochem 2018;123:17–26.
[46] Kim S, Stanford LA, Rodgers RP, Marshall AG, Walters CC, Qian K, et al. Microbial alteration of the acidic and neutral polar NSO compounds revealed by Fourier transform ion cyclotron resonance mass spectrometry. Org Geochem 2005;36:1117–34.
[47] de Aguiar DVA, Da Silva LG, Da Silva RR, Júnior IM, Gomes ADO, Mendes LAN, et al. Comprehensive composition and comparison of acidic nitrogen- and oxygen-containing compounds from pre- and post-salt Brazilian crude oil samples by ESI (-) FT-ICR MS. Fuel 2022;326:125129.
[48] Wang D, Li M, Cheng D, Du Y, Shi Q, Zou X, et al. New biodegradation degree proxies based on acids and neutral nitrogen- and oxygen-containing compounds characterized by high resolution mass spectrometry. Fuel 2023;347:128438.
[49] Shi Q, Hou D, Chung KH, Xu C, Zhao S, Zhang Y. Characterization of Heteroatom Compounds in a Crude Oil and Its Saturates, Aromatics, Resins, and Asphaltenes (SARA) and Non-basic Nitrogen Fractions Analyzed by Negative-Ion Electrospray Ionization Fourier Transform Ion Cyclotron Resonance Mass Spectrometry. Energy Fuels 2010;24:2545–53.
[50] Volkman JK, Jeffrey SW, Nichols PD, Rogers GI, Garland CD. Fatty acid and lipid composition of 10 species of microalgae used in mariculture. J Exp Mar Biol Ecol 1989;128:219–40.
[51] Li Z, Huang H, Zhang S. The effect of biodegradation on bound biomarkers released from intermediate-temperature gold-tube pyrolysis of severely biodegraded Athabasca bitumen. Fuel 2020;263:116669.
[52] Barros EV, Filgueiras PR, Lacerda V, Rodgers RP, Romão W. Characterization of naphthenic acids in crude oil samples – A literature review. Fuel 2022;319:123775.
[53] Hughey CA, Galasso SA, Zumberge JE. Detailed compositional comparison of acidic NSO compounds in biodegraded reservoir and surface crude oils by negative ion electrospray Fourier transform ion cyclotron resonance mass spectrometry. Fuel 2007;86:758–68.
[54] Tomczyk NA, Winans RE, Shinn JH, Robinson RC. On the nature and origin of acidic species in petroleum. 1. Detailed acid type distribution in a California crude oil. Energy Fuels 2001;15:1498–504.
[55] Nojiri H, Nam JW, Kosaka M, Morii KI, Takemura T, Furihata K, et al. Diverse oxygenations catalyzed by carbazole 1,9a-dioxygenase from Pseudomonas sp. Strain CA10. J Bacteriol 1999;181:3105–13.
[56] Ouchiyama N, Zhang Y, Omori T, Kodama T. Biodegradation of Carbazole by Pseudomonas spp. CA06 and CA10. Biosci Biotech Bioch 1993;57:455–60.
[57] Sato SI, Nam JW, Kasuga K, Nojiri H, Yamane H, Omori T. Identification and characterization of genes encoding carbazole 1,9a-dioxygenase in Pseudomonas sp. strain CA10. J Bacteriol 1997;179:4850–8.
[58] Sato SI, Ouchiyama N, Kimura T, Nojiri H, Yamane H, Omori T. Cloning of genes involved in carbazole degradation of Pseudomonas sp. strain CA10: nucleotide sequences of genes and characterization of meta-cleavage enzymes and hydrolase. J Bacteriol 1997;179:4841–9.